Effect of pressure on magnetic properties of MnBi prepared by low-temperature liquid phase sintering

Satienrapong Ngamsomrit[1], Tanachat Eknapakul[2], Supree Pinitsoontorn[3] and Prayoon Songsiriritthigul[1,2*]

Abstract

In this work, manganese bismuth (MnBi) magnetic powders were synthesized by low-temperature liquid phase sintering in three different base pressures: ultra-high vacuum (UHV, P≈10^{-8} mbar), low vacuum (LV, P≈10^{-2} mbar) and ambient pressure (AP). The MnBi powders were successfully prepared at 375 ^{o}C for 12 hrs with a 1:1 (Mn:Bi) atomic ratio. The magnetic properties of the sintered MnBi samples were studied using a vibrating sample magnetometer (VSM). The coercivity, saturation magnetization value (M_s) and maximum energy product ($(BH)_{max}$) of up to 2.42±0.07 kOe, 48.46±0.9 emu/g and 1.82±0.05 MGOe, respectively, were obtained in the MnBi sintered in ultra-high vacuum (UHV-MnBi). The morphology and chemical composition of MnBi powders were examined by scanning electron microscope (SEM) combined with energy dispersive x-ray spectroscopy (EDS). It was found that the sample sintered in ambient pressure was inhomogeneous with noticeably separated layers of Bi, Mn and MnBi, while the UHV-MnBi ingot was relatively homogeneous. The sintered products, i.e., MnBi, Bi and MnO were revealed by using x-ray diffraction. Three types of oxides which are MnO, α-MnO_2 and β-MnO_2 were found in all samples with different proportions and ratios. Finally, more homogenous particles with relatively less oxides were obtained in the UHV-MnBi, which are two main requirements to acquire high $(BH)_{max}$.

Keywords: manganese bismuth (MnBi), low-temperature sintering, maximum energy product ($(BH)_{max}$)

[1] Suranaree University of Technology and Synchrotron Light Research Institute

[2] Thailand Center of Excellence in Physics, MHESRI

[3] Institute of Nanomaterials Research and Innovation for Energy, Khon Kaen University

[*] Corresponding author. E-mail: py.song@sut.ac.th

Received: March 14, 2022; Revised: May 5, 2022; Accepted: June 8, 2022

Introduction

The demand for rare-earth-based products, especially permanent magnets, is increasing in everyday life, which is in contrast to their reduced amount known as the 'rare-earth crisis (Gutfleisch et al., 2011; Li et al., 2018a). This brings the attention of researchers to find alternatives to solve this problem. Nowadays, there are extensive studies on rare-earth free permanent magnet (Poudyal, & Liu, 2013). Among them, MnBi is a potential candidate which attracted both theoretical and experimental studies due to its outstanding magnetic features such as positive temperature coefficient and high curie temperatures (Yang et al., 2002a; Cui, et al., 2014a). Its theoretical maximum energy product ($(BH)_{max}$) is of 17.6 MGOe (Nguyen et al., 2014). The highest experimental $(BH)_{max}$ to date of up to 13 MGOe were reported in the arc-melted MnBi following by a single-step annealing and 8 hr. ball milling (Jensen et al., 2019). In practice, it is very difficult to obtain high purity and a single phase of MnBi through general techniques, i.e., arc-melting and sintering (Cui, et al., 2014b). Moreover, the magnetic performance of MnBi is sensitive to particle size, morphology, MnBi contents, and oxides which are associated with the preparation methods, production procedure, and the managed environment (Rao, & Hadjipanayis, 2015).

Nowadays, MnBi magnets can be synthesized by various approaches such as arc-melting (Huang, Shi, Hou, & Cao, 2019) melt-spinning (Liu, Wang, & Dong, 2018) chemical methods (Sun et al., 2016) and sintering (Ngamsomrit et al., 2021; Borsup et al., 2022). However, it is still challenging to scale up for mass production either by the difficulty of post-sintering processes or time consuming (Yang et al., 2002b). Recently, we have published the formation and magnetic properties of low-temperature phase manganese bismuth prepared by low-temperature liquid phase sintering in vacuum, which requires fewer post-sintering processes, lower energy and time consumption. Overall processes can be finished within three days using thermal annealing below 340 °C, which is higher than the Bi melting point but lower than peritectic temperature (Cao et al., 2018). However, we realized that this ultra-high vacuum sintering process is still not applicable on an industrial scale.

In this work, we are searching a way to produce MnBi in the industrial scale by tuning down the operating pressure. The MnBi samples were successfully prepared in ultra-high vacuum (UHV), low vacuum (LV) and ambient pressure (AP). The prepared samples were characterized by x-ray diffraction (XRD) and scanning electron microscopy (SEM) combined with energy

dispersive spectroscopy (EDS). The evolution of their magnetic properties was studied by using a vibrating sample magnetometer (VSM).

Methodology

In this study, the sintered MnBi samples were prepared in two different systems. The ultra-high vacuum (UHV) MnBi were prepared using a vacuum sintering system. The low vacuum (LV) and ambient pressure (AP) MnBi were prepared in a tube furnace. The target pressures of the UHV, LV and AP are 10^{-8}, 10^{-2} mbar and 1 bar, respectively. The starting materials were Mn powder (99+% purity, 40 mesh (<420 μm)) and Bi powder (99.5% purity, 100 mesh (<149 μm)) supplied by Acros Organics. Mn particle powders were obtained using the planetary mill for 3 hrs and then sieved screen Mn powders of less than 20 μm. Afterward, the chosen Mn and Bi powders were mixed in a 1:1 atomic ratio and then loaded into a quartz crucible of the low-temperature effusion cell (Dr. Eberl MBE-Komponenten GmbH, Germany) for the UHV system. For the LV system, the samples were loaded into a quartz tube (60 mm (OD) × 52 mm (ID) × 1.2 m, 4 mm (T)). The temperature of both systems was gradually increased with 5 ^{o}C/min rate. The specimens were sintered at 375 ^{o}C for 12 hrs and are labeled as UHV-MnBi (ultra-high vacuum), LV-MnBi (low vacuum) and AP-MnBi (ambient pressure) depending on their sintering pressures. The morphology and elemental composition of MnBi powders were examined by scanning electron microscope (SEM) combined with energy-dispersive x-ray spectroscopy (EDS) (Quanta 450). The phase identification was investigated using X-ray diffraction (XRD, Bruker D2 Phaser, Cu K_{α} radiation, λ=1.5406 Å). The magnetic properties were measured by using a vibrating sample magnetometer (VSM, Quantum Design, VersaLab).

Results and discussion

1. Phase identification

The preparation of high-purity MnBi magnetic materials with high energy product ($(BH)_{max}$) is interesting because its magnetic properties depend sensitively on microstructure, concentration and morphology correlating to the preparation method and controlled environment (Chen et al., 2016; Poudyal et al., 2016). The formation of MnBi magnetic materials at a temperature higher than the Bi melting point influences on the rearrangement of Mn particles in liquid of Bi known as liquid - solid interactions (Corbin, & McIsaac, 2003). One of the difficulties in synthesizing LTP-MnBi is the fact that Mn reacts with oxygen rapidly forming several oxides. Other important factors are the phase-change reactions during temperature increasing/ decreasing such as peritectic reaction which is

the reaction between solid and liquid phase resulting in a new solid phase. This reaction usually takes place during sintering process. Moreover, the eutectic reaction could also be occurred while cooling the liquid phase giving two new solid phases. In case of MnBi, it can be explained that while reducing the temperature, the separation between MnBi and Bi occurs. This reveals an excess of Bi which largely reduces its magnetic performance during preparation process (Oikawa, Mitsui, Koyama, & Anzai, 2011; Cui et al., 2014a).

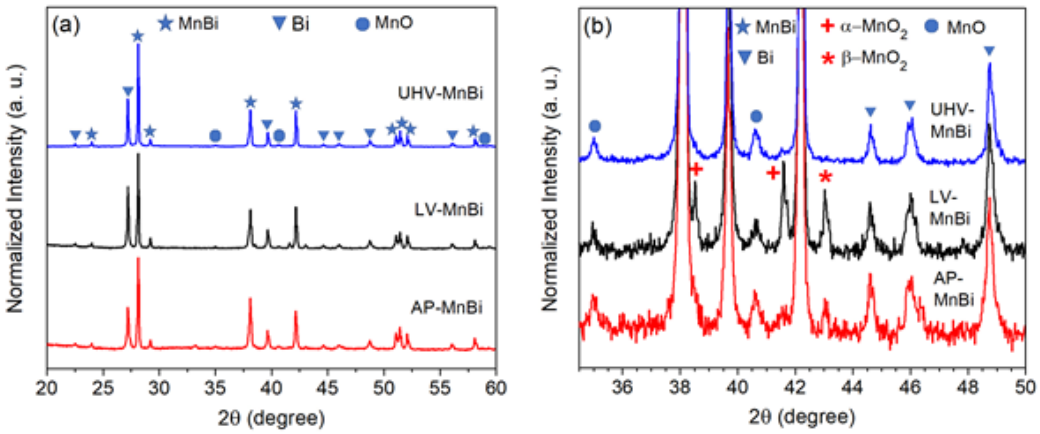

Figure 1 (a) XRD patterns of UHV-MnBi, LV-MnBi and AP-MnBi samples and (b) Zoom-in of (a) between the 2-theta range of 34.5°- 50.0°.

The samples sintered at different pressures were categorized by base pressure denoted as ultra-high vacuum (UHV, (10^{-8} mbar)), low vacuum (LV, (10^{-2} mbar)), and ambient pressure (AP, (1 bar)). (Figure 1a) shows the wide scan XRD patterns of all MnBi powders whose main diffraction peaks could be identified as MnBi phase (JCPDS Card. No. 96-900-8900), Bi phase (JCPDS Card. No. 01-085-1329), cooperated with small peaks of Manganese oxides (MnO; JCPDS Card. No. 96-101-0394, **α**-MnO_2; JCPDS Card. No. 44-0141 and **β**-MnO_2; JCPDS Card. No. 024-0735). The MnBi/(MnBi+Bi) ratio extracted from the XRD peaks were calculated to be 54.90, 54.50 and 70.60% for UHV-MnBi, LV-MnBi and AP-MnBi, respectively. It should be noted that this ratio does not fully represent the MnBi concentration in the sample. Since, the Mn peaks could not be detected due to the limit of X-ray penetration. It could be implied that the MnBi concentration in the Mn-rich AP-MnBi (the sample was taken from the MnBi (black) region shown in (Figure 3a)

might be far less than this value. As expected, the oxidation rate depends on the oxygen partial pressure during sintering (Li et al., 2018b) and thus, the lowest amount of oxides is observed for the UHV-MnBi. It is noted that α-MnO_2 and β-MnO_2 are pronounced for the sample sintered in a low vacuum, i.e. LV-MnBi sample. These oxides are formed on the surface of the MnBi powder particles. The quantitative comparison of surface oxides composition could be further investigated by the XPS technique.

2. Magnetic properties

Firstly, the M-H curves were corrected by using a demagnetization factor (N) which is dependent on the shape and orientation of the ferromagnetic materials to the external field. This can be calculated by, $N^{-1} = 2 + \frac{1}{\sqrt{2}}\frac{a}{b}$, according to the transverse-cylindrical geometry (Prozorov, & Kogan, 2018). The N value of 0.4 was calculated from $\frac{a}{b} = \frac{1}{\sqrt{2}}$, where a is a length and b is a diameter of the sample. (Figure 2a) shows the room temperature hysteresis loop of the sintered MnBi specimens prepared at 375 °C for 12 hrs under ultra-high vacuum (UHV), low vacuum (LV), and ambient pressure (AP). The changes of demagnetization curves of raw M (N=0) and corrected M (N=0.4) of UHV-MnBi are seen in the bottom-right inset of (Figure 2a). The magnetic measurements were repeated 3 times in each sample giving the corrected H_c of 2.42±0.07, 0.68±0.06, 0.87±0.04 kOe and M_s of 48.46±0.90, 56.54±0.95, 49.80±0.66 emu/g for UHV-MnBi, LV-MnBi and AP-MnBi samples, respectively summarized in (Table 1). It should be noted that the UHV-MnBi exhibits the hard magnetic behavior with up to 3.50 times of H_c compared to LV-MnBi and AP-MnBi. Even the slightly less Ms value of UHV-MnBi (up to 14% compared to the LV-MnBi) consistent with the observed MnBi concentration measured from XRD, the UHV-MnBi remains the highest $(BH)_{max}$ of 1.82±0.05 MGOe among others which is due to its notably high H_c as shown in (Figure 2b).

3. Morphology

(Figures 3a and 3e) show the physical appearances of AP-MnBi and UHV-MnBi ingot obtained immediately after the sintering process. It is clearly seen that the AP-MnBi is inhomogeneous with noticeably separated layers of Bi (white region) and MnBi (black region) which are shown in the inset of (Figure 3a), while the UHV-MnBi ingot is relatively homogeneous. It is understood that the formation of forming MnBi by a chemical reaction at the liquid phase sintering (LPS) (German, Suri, & Park, 2009) and atmospheric pressure. Initially, the Bi liquid reacts with Mn particle powders to form a MnBi layer coating Mn inner core. Moreover, the atmospheric pressure is an important factor that suppresses the MnBi formation due to the oxide formation. The high-resolution SEM images of

AP-MnBi ingot are shown in (Figure 3b). It is confirmed that the surface composition is inhomogeneous, as shown in the EDS results in (Figure 3c and 3d). It was found that the top area and surface of the as-sintered AP-MnBi are Bi-rich and oxygen-rich (Yoshida, Shima, & Takahashi, 1999). This could be explained by the incomplete formation and hindering of the MnBi phase during sintering in the ambient condition either by the formation of oxides or peritectic reaction. The Mn:Bi:O ratio of 40.8:33.6:21.2 and 16.2:67.2:10.4 %wt were observed in the black and white regions of AP-MnBi. While the ratio of 45.2:44:4.9 and 33.2:54.1:9.2 were carried out from region 1 and 2 of the UHV-MnBi. This result strongly confirms the more homogeneous and less oxides coverage of the UHV-MnBi than AP-MnBi.

Table 1 Magnetic properties of all sintered samples.

samples	H_c (kOe)	M_s (emu/g)	$(BH)_{max}$ (MGOe)
UHV-MnBi	2.42±0.07	48.46±0.90	1.82±0.05
LV-MnBi	0.68±0.06	56.54±0.95	1.47±0.08
AP-MnBi	0.87±0.04	49.80±0.66	0.92±0.04

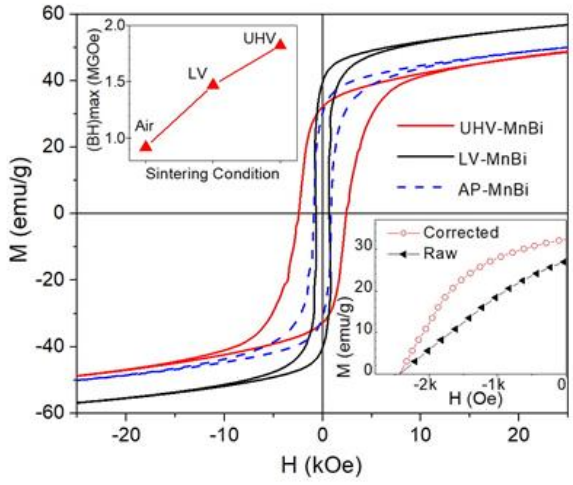

Figure 2 (a) M-H curves after demagnetizing field correction of UHV-MnBi, LV-MnBi and AP-MnBi. The inset of (a) shows the demagnetization curves of raw M (N=0) and correct M (N=0.4) of the UHV-MnBi (bottom-right) and (b) shows the maximum energy product ($(BH)_{max}$) of all samples.

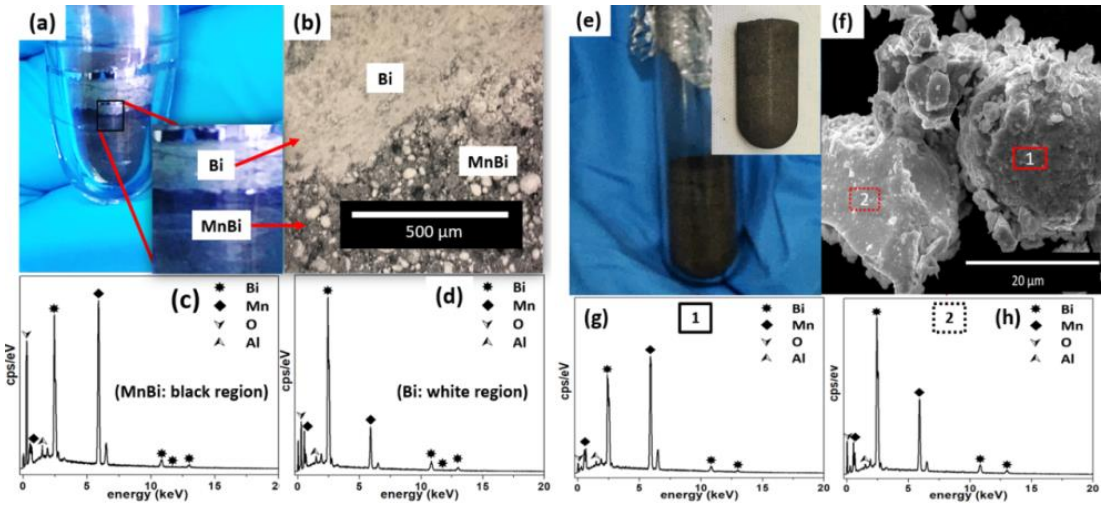

Figure 3 (a) camera image (b) high-resolution SEM images (c) EDS spectra taken at MnBi region (black region) and (d) Bi region (white) of AP-MnBi ingot (e) camera image (f) high-resolution SEM images (g) EDS spectra taken at region 1 and (h) region 2 of UHV-MnBi ingot.

Conclusion

This work demonstrates the success in preparing MnBi in ultra-high vacuum, low vacuum, and ambient pressure. The vacuum pressure plays an important role in the formation of MnBi during liquid phase sintering (LPS). After the sintering process, the AP-MnBi ingot is inhomogeneous, containing the separated layers of Bi and MnBi, while the UHV-MnBi ingot is rather homogeneous. The formation of different kinds of oxides is found in LV-MnBi and AP-MnBi more than in UHV-MnBi. Thus, it could be concluded that the inhomogeneity and oxides play an important role in the magnetic properties of MnBi. UHV-MnBi presented the highest $(BH)_{max}$ of up to 1.82±0.05 MGOe. Finally, we showed here that the MnBi can be prepared even in atmospheric pressure. However, further studies and system optimization are required to obtain acceptable magnetic performance.

Acknowledgement

This work has been partially supported by the Thailand Center of Excellence in Physics and Research Network NANOTEC program of the National Nanotechnology Center of Thailand.

References

Borsup, J., Eknapakul, T., Myint, H. T., Smith, M. F., Yordsri, V., Pinitsoontorn, S., & Songsiriritthigul, P. (2022). Formation and magnetic properties of

low-temperature phase manganese bismuth prepared by low-temperature liquid phase sintering in vacuum. *Journal of Magnetism and Magnetic Materials*, *544*, 168661.

Cao, J., Huang, Y. L., Hou, Y. H., Zhang, G. Q., Shi, Z. Q., Zhong, Z. C., & Liu Z. W. (2018). Effect of intergranular phase on the coercivity for MnBi magnets prepared by spark plasma sintering. *AIP Advances, 8*, 055132.

Chen, Y. C., Sawatzki, S., Ener, S., Sepehri-Amin, H., Leineweber, A., Gregori, G., Qu, F., Muralidhar, S., Ohkubo, T., Hono, K., Gutfleisch, O., Kronmüller, H., Schütz, G., & Goering, E. b. (2016). On the synthesis and microstructure analysis of high performance MnBi. *AIP Advances*, *6,* 125301.

Corbin, S. F., & McIsaac, D. J. (2003). Differential scanning calorimetry of the stages of transient liquid phase sintering. *Materials Science Engineer A, 346*, 132-140.

Cui, J., Choi, J. P., Li, G., Polikarpov, E., Darsell, J., Overman, N., Olszta, M., Schreiber, D., Bowden, M., Droubay, T., Kramer, M., Zarkevich, N. A., Wang, L. L., Johnson, D. D., Marinescu, M., Takeuchi, I., Huang, Q. Z., Wu, H., Reeve, H., Vuong, N. V., & Liu, J. P. (2014). Thermal stability of MnBi magnetic materials. *Journal of Physics: Condensed Matter, 26*, 064212.

Cui, J., Choi, J. P., Li, G., Polikarpov, E., Darsell, J., Kramer, M., Zarkevich, N. A., Wang, L. L., Overman, N., Johnson, D. D., Marinescu, M., Huang, Q. Z., Wu, H., Vuong, N. V., & Liu, J. P. (2014). Development of MnBi permanent magnet: Neutron diffraction of MnBi powder. *Journal of Applied, 115*, 17A743.

German, R. M., Suri, P., & Park, S. J. (2009). Review: liquid phase sintering. *Journal of Materials Science, 44,* 1-39.

Gutfleisch, O., Willard, M. A., Bruck, E., Chen, C. H., Sankar, S. G., & Liu, J. P. (2011). Magnetic materials and devices for the 21st century: stronger, lighter, and more energy-efficient. *Advanced Materials*, *23*, 821-842.

Huang, Y. L., Shi, Z. Q., Hou, Y. H., & Cao, J. (2019). Microstructure, improved magnetic properties, and recoil loops characteristics for MnBi alloys. *Journal of Magnetism and Magnetic Materials, 485,* 157-164.

Jensen, B. A., Tang, W., Liu, X., Nolte, A. I., Ouyang, G., Dennis, K. W., & Cui, J. (2019). Optimizing composition in MnBi permanent magnet alloys. *Acta Materialia, 181*, 595-602.

Li, B., Ma, Y., Shao, B., Li, C., Chen, D., Sun, J., Zheng, Q., & Yin, X. (2018a). Preparation and magnetic properties of anisotropic MnBi powders. *Physica B: Condensed Matter*, *530*, 322-326.

Li, C., Guo, D., Shao, B., Li, K., Li, B., & Chen, D. (2018b). Effect of heat treatment and ball milling on MnBi magnetic materials. *Materials Research Express, 5*, 016104.

Liu, S., Wang, J., & Dong, F. (2018). A new bottom-up synthesis of MnBi particles with high magnetic performance. *Chemical Physics Letter, 691*, 325-329.

Ngamsomrit, S., Saisopa, T., Borsup, J., Tun, M. S., Myint, H. T., Nakajima, H., Songsiriritthigul, C., Pinitsoontorn, S., & Songsiriritthigul, P. (2021). Preparation of low-temperature phase MnBi by sintering in vacuum. *Journal of Physics: Conference Series, 1719*(1), 012057.

Nguyen, V. V., Poudyal, N., Liu, X., Liu, J. P., Sun, K., Kramer, M. J., & Cui, J. (2014). High-performance MnBi alloy prepared using profiled heat treatment. *IEEE Transactions on Magnetics, 50*(12), 2105506.

Oikawa, K., Mitsui, Y., Koyama, K., & Anzai, K. (2011). Thermodynamic assessment of the Bi-Mn system. *Materials Transactions, 52*, 2032-2039.

Poudyal, N., & Liu, J. P. (2013). Advances in nanostructured permanent magnets research. *Journal of Physics D: Applied Physics, 46*, 043001.

Poudyal, N., Liu, X., Wang, W., Nguyen, V. V., Ma, Y., Gandha, K., Elkins, K., Liu, J. P., Sun, K., Kramer, M. J., & Cui, J. (2016). Processing of MnBi bulk magnets with enhanced energy product. *AIP Advances, 6*, 056004.

Prozorov, R., & Kogan, V. G. (2018). Effective demagnetizing factors of diamagnetic samples of various shapes. *Physical Review Applied, 10*, 014030.

Rao, N. V. R., & Hadjipanayis, G. C. (2015). Influence of jet milling process parameters on particle size, phase formation and magnetic properties of MnBi alloy. *Journal of Alloys and Compounds, 629*, 80-83.

Sun, J., Li, C., Huang, Q., Liu, G., Han, G., Yu, S., & Kang, S. (2016). A facile way to synthesize rare-earth-free Mn-Bi@Bi magnetic nanoparticles. *RSC Advances, 6*, 100035-100039.

Yang, J. B., Yelon, W. B., James, W. J., Cai, Q., Kornecki, M., Roy, S., Ali, N., & Heritier Ph. I. (2002a). Crystal structure, magnetic properties and electronic structure the MnBi intermetallic compound. *Journal of Physics: Condensed Matter*, *14*, 6509-6519.

Yang, J. B., Yelon, W. B., James, W. J., Cai, Q., Roy, S., & Ali, N. (2002b). Structure and magnetic properties of the MnBi low temperature phase. *Journal of Applied Physics, 91*(10), 7866-7868 .

Yoshida, H., Shima, T., & Takahashi, T. (1999). Preparation of highly pure MnBi intermetallic compounds by Arc-Melting. *Materials Transaction, JIM, 40*, 455-459.